Nano Energy 53 (2018) 168–174

Contents lists available at ScienceDirect

Nano Energy

journal homepage: www.elsevier.com/locate/nanoen

Communication

Stabilizing interface between $Li_{10}SnP_2S_{12}$ and Li metal by molecular layer deposition

Changhong Wang[a], Yang Zhao[a], Qian Sun[a], Xia Li[a], Yulong Liu[a], Jianwen Liang[a], Xiaona Li[a], Xiaoting Lin[a], Ruying Li[a], Keegan R. Adair[a], Li Zhang[b], Rong Yang[b], Shigang Lu[b], Xueliang Sun[a,*]

[a] Department of Mechanical and Materials Engineering, University of Western Ontario, 1151 Richmond St, London, Ontario N6A 3K7, Canada
[b] China Automotive Battery Research Institute Co., Ltd, 5th Floor, No. 43, Mining Building, North Sanhuan Middle Road, Haidian District, Beijing 100088, China.

ARTICLE INFO

Keywords:
All-solid-state lithium metal battery
Molecular layer deposition
Sulfide electrolyte
Li metal interface

ABSTRACT

Safe and high-energy-density lithium rechargeable batteries are urgently required for vehicle electrification and grid energy storage. All-solid-state lithium metal batteries (ASSLMBs) are regarded as a good choice to meet these stringent requirements. However, interfacial instability between Li metal and solid-state sulfide electrolytes (SEs) and lithium dendrite formation are main challenges to be overcome. In this work, molecular layer deposition (MLD) is employed for the first time to develop an inorganic-organic hybrid interlayer (alucone) at the interface between the Li metal and SEs. It is found that the alucone layer can serve as an artificial solid electrolyte interphase (SEI). As a result, interfacial reactions between Li and SEs are significantly suppressed by intrinsically blocking electron transfer at the interface. In addition, lithium dendrites are also suppressed. Coupled with a $LiCoO_2$ cathode, ASSLMBs with 30 MLD cycles of alucone on Li metal exhibit a high initial capacity of 120 mAh g^{-1} and can retain a capacity of 60 mAh g^{-1} after 150 cycles. This work exemplifies the use of MLD to stabilize the interface between SEs and Li metal for ASSLMBs.

1. Introduction

All-solid-state lithium metal batteries (ASSLMBs) have gained increasing interest in recent years due to their superior safety and higher energy density over those of state-of-the-art lithium-ion batteries. [1,2] To realize ASSLMBs, the development of solid-state electrolytes is essential. Currently, there are three main categories of solid-state electrolytes under development, including lithium-ion-conductive polymer electrolytes, inorganic lithium-ion-conductive ceramics and their composites as hybrid electrolytes. [3,4] Among the inorganic ceramics, sulfide electrolytes (SEs) are attracting increasing interest due to their outstanding ionic conductivity ($> 10^{-3}$ S/cm). For example, $Li_{9.54}Si_{1.74}P_{1.44}S_{11.7}Cl_{0.3}$ shows an ionic conductivity of 25 mS cm^{-1}, [5] which is almost two times higher than that of conventional liquid electrolytes (10.2 mS cm^{-1}). [6] On the other hand, Li metal is considered as the ultimate choice among all the possible anodes for solid-state lithium batteries due to its highest theoretical capacity of 3860 mAh g^{-1}, or 2061 mAh cm^{-3} and lowest electrochemical potential (–3.040 V versus the standard hydrogen electrode), ASSLMBs with high energy density can be achieved. [4,7,8]

However, two major challenges hinder the direct use of Li metal in ASSLMBs. Firstly, lithium dendrite formation can lead to short circuiting and poses serious safety concerns. Secondly, the interface instability between Li metal and SEs leads to large interfacial resistance for Li-ion (Li^+) conduction. Over the past decades, several promising strategies have been proposed to enable the use of Li metal in ASSLMBs: (1) using Li-Metal alloys instead of pure Li metal anodes, such as Li-In and Li-Al alloys. [9,10] (2) double layer electrolytes with distinct properties, in which using relatively stable SEs against Li metal can improve the interfacial stability, [11,12] and (3) protective layers on the Li metal surface, [13–15] such as LiH_2PO_4 [16] and Al_2O_3, [17] to engineer the interface. However, many of these strategies have drawbacks such as sacrificing the electrochemical potential of Li metal, lowering the overall energy density, and difficulty in achieving uniform thin film coatings.

In this work, we use molecular layer deposition (MLD) for the first time to develop an inorganic-organic hybrid interlayer (alucone) at the interface between the SEs and Li metal. It was found that the alucone layer can serve as an artificial solid electrolyte interphase (SEI), intrinsically blocking the electron transfer at the anode interface, thus completely suppressing the interfacial reactions between Li and SEs. Moreover, lithium dendrite formation was also suppressed by the MLD

* Corresponding author.
E-mail address: xsun9@uwo.ca (X. Sun).

https://doi.org/10.1016/j.nanoen.2018.08.030
Received 9 July 2018; Received in revised form 13 August 2018; Accepted 15 August 2018
Available online 21 August 2018

coating. In light of the molecular structure of coatings, the inorganic-organic hybrid MLD coating has improved mechanical properties over that of purely inorganic coatings such as Al_2O_3, which is beneficial for the accommodation of the stress/strain caused by the volume change of electrodes. Coupled with a $LiCoO_2$ cathode, ASSLMBs with the Li metal protected by alucone exhibit smaller polarization, higher capacity, and longer cycle life than those with bare Li metal. The underlying reasons are believed to be the suppression of interfacial reactions and lithium dendrite formation, thus guaranteeing the long-term cyclability of ASSLMBs. This work exemplifies the use of MLD to stabilize the interface between SEs and Li for ASSLMBs.

2. Experimental section

2.1. Li preparation

A fresh Li foil was used directly. Molecular layer deposition (MLD) of Alucone coatings were conducted in a Gemstar-8 ALD system (Arradiance, USA) directly connected with the argon-filled glove box. Alucone was directly deposited on the as-prepared foil at 85 ℃ by alternatively introducing trimethylaluminum (TMA) and ethylene glycol (EG) as precursors. The MLD process is performed as a sequence of TMA pulse/purge/EG pulse/purge sequence with the time of 0.01 s/40 s/0.01 s/70 s, respectively. The different cycle numbers of 10, 30 and 50 MLD alucone coating on Li foils are named 10alucone Li, 30alucone Li, and 50alucone Li, respectively. For comparison, Al_2O_3 was performed using TMA and H_2O as precursors at 85 ℃ by ALD.

2.2. Electrochemical measurements

The electrochemical analysis was performed in CR2032 coin-type cells. $Li_{10}SnP_2S12$ was purchased from NEI corporation. The symmetric cells with a configuration of Li/$Li_{10}SnP_2S_{12}$/Li were assembled in an ultra-pure argon-filled glove box. The Li stripping/plating studies were carried out in an Arbin BT-2000 battery test system at room temperature. Constant current densities were applied to the electrodes during repeated stripping/plating while the potential was recorded over time. Electrochemical impedance analysis was performed on a biologic electrochemical station with a frequency range from 1000 kHz to 100 m Hz with an amplitude of 10 mV. Cathode composites were mixed with $LiCoO_2$, $Li_{10}SnP_2S_{12}$, and acetylene black with a ratio of 60:34:6. To assemble all-solid-state lithium metal batteries, the 80 mg $Li_{10}SnP_2S_{12}$ were pelletized under 1 t using a pelletizer with a diameter of 1/2 in. Then 10 mg cathode composites were put on the side of $Li_{10}SnP_2S_{12}$ and then pressed at 3 t. Finally, Li foil was put on another side of $Li_{10}SnP_2S_{12}$ and pressed at 0.5 t. All the ASSLMBs were tested with the cut-off voltages from 2.5 V to 4.5 V.

2.3. Characterizations

The morphology of materials was analyzed by a Hitachi S-4800 field emission SEM equipped with EDX. XRD patterns were scanned using a Bruker D8 diffractometer, using Cu Kα radiation. X-ray photoelectron spectroscopy was performed using Thermo Scientific ESCALAB 250Xi with Al Kα-radiation. The pressure in the analysis chamber was typically 2×10^{-9} Torr during acquisition. Raman spectra were collected using the laser with a wavelength of 532 nm.

3. Results and discussion

The configuration of all-solid-state lithium metal batteries (ASSLMBs) is illustrated in Fig. 1a, which is consisted of Li metal, SEs, and a cathode. Generally, once bare Li directly contacts with SEs, a resistive layer forms at the interface due to the chemical instability of SEs against highly reactive Li metal (Fig. 1b). [16,18] Here, we employed MLD to introduce an inorganic-organic hybrid thin film (alucone) at the interface (Fig. 1c). The chemical structure of polymeric alucone films is present in Fig. 1d, which was deposited on the Li surface by MLD using the precursors of trimethylaluminum (TMA) and ethylene glycol (EG). [19,20] The morphology of Li foils was checked by scanning electron microscopy (SEM). As shown in Fig. S1, there is no obvious change on the Li metal surface after the MLD process. X-ray photoelectron spectroscopy (XPS) was used to confirm the alucone thin film the Li surface, Al, Li, C, and O peaks were clearly detected on the Li surface after 30 MLD cycles (Fig. S2), which are originated from the polymeric alucone layer. It should be mentioned that the thickness of the MLD thin film can be controlled at the atomic/molecular level through the self-limiting reactions between two precursors. Based on our previous study, the growth rate of alucone on Li metal foils is 0.3–0.5 nm per cycles. [20,21] The different thickness of the alucone coating on Li metal is listed in Table S1. Detailed MLD coating process can be found in the experimental section. The alucone thin film has the abundant ether bond (–O–), which is effectively helpful for Li^+ transport, [22] thus serving as an artificial solid-electrolyte interphase (SEI) on Li surface after lithiation. SEI is known as a good lithium-ion conductor but electronic insulator. [23] Thus interfacial reactions between Li metal and SEs could be suppressed by blocking electron transfer between Li and SEs. Furthermore, MLD coatings generally have a lower elastic modulus than pure inorganic coatings, which is beneficial for the accommodation of stress/strain caused by the volume change of electrodes during cycling. [20,21,24]

In terms of SEs, a member of LMPS family-$Li_{10}SnP_2S_{12}$ (LSPS)-was selected, which is favorable for its satisfactory ion conductivity and low cost for practical application. [25–27] The crystal structure framework of LSPS consists of $(Sn_{0.5}P_{0.5})S_4$ tetrahedra, PS_4 tetrahedra, LiS_6 octahedra, and LiS_4 tetrahedra (Fig. 2a and Fig. S3). [25,26] LSPS has a one-dimensional conduction path along the c-axial. [28] In addition, the *thio*-LiSICON structure of LSPS is evidenced by X-ray diffraction (XRD) patterns (Fig. 2b). Based on the electrochemical impedance spectroscopy (EIS) measurement, the ionic conductivity of $Li_{10}SnP_2S_{12}$ is 3.12×10^{-4} S/cm at the room temperature (Fig. 2c). According to the Nernst-Einstein equation $\sigma(T) = A\exp(-E_A/k_BT)$, where σ is the ionic conductivity at a certain temperature, A is the pre-exponential factor, T is the temperature in Kelvin, k_B as the Boltzmann constant, E_A is the activation energy of Li^+ hopping between two adjacent sites, [29] LSPS possesses an activation energy of 0.285 eV (Fig. 2d). In addition, the morphology of LSPS was also examined by scanning electron microscopy (SEM) (Fig. S4). The particle size of LSPS varies from a few hundred nanometers to several micrometers. The large particle seems to be the aggregation of the small LSPS particles.

By co-axial pressing, LSPS can be easily pressed into pellets because of its low elastic modulus. Furthermore, to evaluate the interface stability between LSPS and Li metal, Li symmetric cells with a structure of Li/LSPS/Li were fabricated and then the EIS was conducted as a function of time. In Nyquist plots of Li symmetric cells, there are two typical EIS spectra. [30,31] One consists of a high-frequency semicircle and a finite-length Warburg impedance at low frequencies (Fig. S5(a)). [30] These characteristics are typical for mixed ion-electron conductor (MCI, an acronym for mixed conductor interphases). Another one is characteristic of a single semicircle at high frequency, which indicates the formation of ion-conducting SEI at the interface (Fig. S5(b)). A detailed explanation is included in the SI. [30] Nyquist plots of Li/LSPS/Li symmetric cells mainly consists of a high-frequency semicircle with a finite-length Warburg impedance (Fig. 3a), which indicates the interface between Li and LSPS is a mixed ion-electron conductor. Both interfacial resistance (Rint) and Warburg impedance (Ws) increase significantly within 24 h, indicating the growth of mixed conductor interphase (MCI) caused by the noticeable interfacial reactions between Li and LSPS. With alucone coating on Li metal, the Nyquist plot mainly shows a single semicircle at the high frequency, indicating that the interface between LSPS and alucone-coated Li metal is an ion-conducting SEI layer (Fig. 3b, c, and d). More interestingly, in the case of

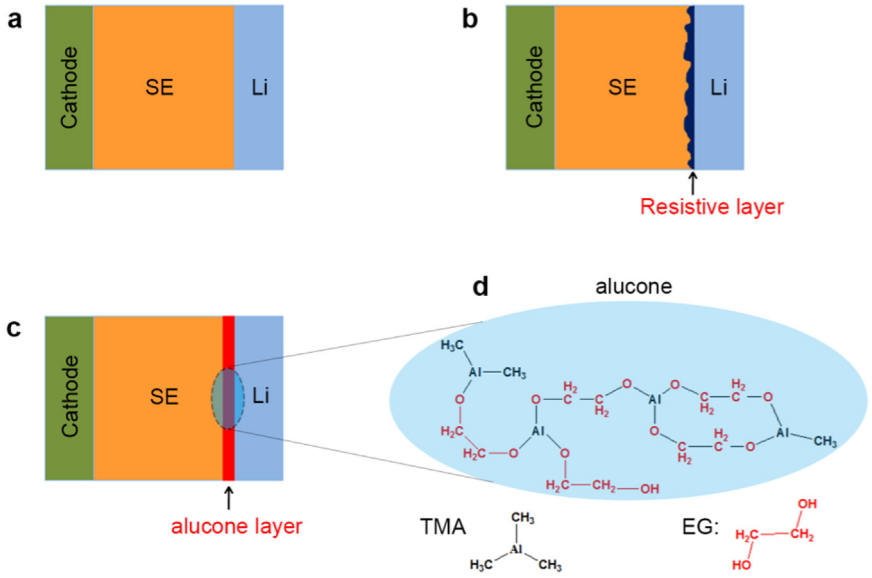

Fig. 1. Schematic illustration of SE-based ASSLMBs. (a) SE-based ASSLMBs. (b) The resistive layer at the interface between Li and SEs. (c) Alucone layer on the Li surface. (d) The chemical structure of alucone deposited by MLD.

10 cycles alucone (10alucone) coating on Li metal, Rint is still increasing within 24 h (Fig. 3b), implying that 10alucone could not completely suppress the interfacial reactions between Li and LSPS. However, in the case of 30 cycles alucone (30alucone) coating on Li metal, Rint is almost stable and the total resistance is minimized (Fig. 3c), indicating that the remarkable interfacial reactions between LSPS and pristine Li are well suppressed. Nevertheless, in the case of 50 cycles alucone (50alucone), the overall resistance is almost 10 K Ohms (Fig. 3d), implying that the thicker alucone coating blocks the ion migration at the interface. From the EIS results, it can be concluded that 30aluocne coating on Li metal can serve as an effective ion-conducting SEI interphase and effectively suppress the interfacial reactions.

Furthermore, to study the electrochemical stability and reversibility of Li metal against LSPS, Li symmetric cells were discharged and charged at a constant current (0.1 mA cm^{-2}) with an areal capacity of 0.1 mAh cm^{-2}. Without any coating, the over-potential of Li^+ platting/stripping is greatly increasing (Fig. 4a), indicating that bare Li metal phenomenally reacts with LSPS, resulting in a highly resistive interphase at the interface. After 4000 min, the over-potential increases to 3.6 V and the short circuit happens, which is related to the unlimited formation of the highly resistive interphase and lithium dendrites. Using 10 cycles alucone coating, the short circuit is suppressed within 10,000 min. However, the over-potential of Li^+ platting/stripping of l0aluocone coated Li is still increased to 3.4 V, which means that 10aluocone coating cannot suppress the interfacial reactions between SEs and Li metal. The plateau of Li^+ platting/stripping at the 1st cycle and 25th cycle are present in Fig. 4b and c, showing the first charge process has a large over-potential at the first cycle, which indicates that Li^+ need to overcome an energy barrier before nucleation. [32] Interestingly, in the case of 30alucone Li, the over-potential of L^{i+} platting/

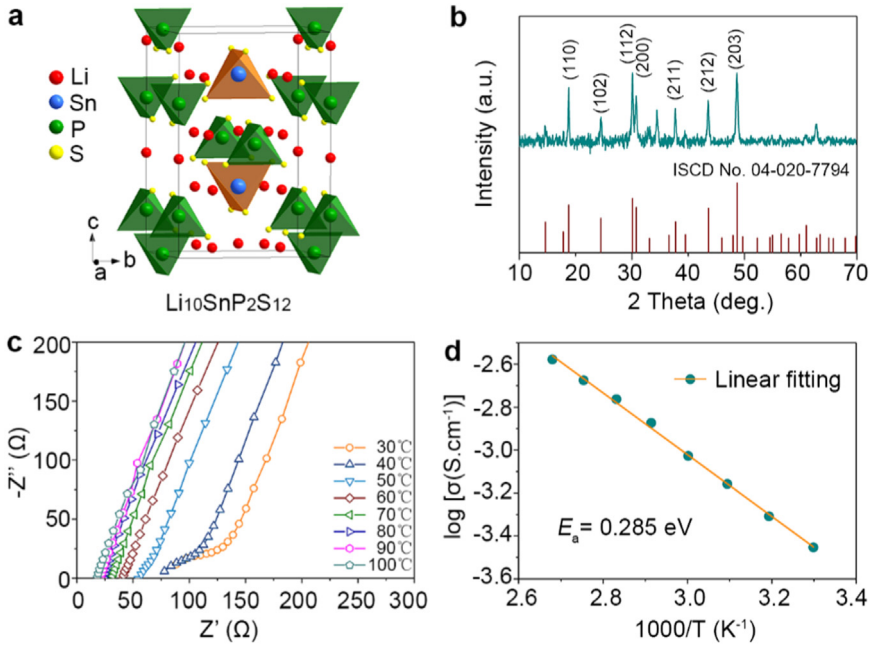

Fig. 2. Characterizations of $Li_{10}SnP_2S_{12}$ (LSPS). (a) Crystal structure of LSPS. (b) XRD pattern of as-prepared LSPS. (c) EIS profiles of LSPS at various temperatures. (d) Arrhenius plot of LSPS conductivity.

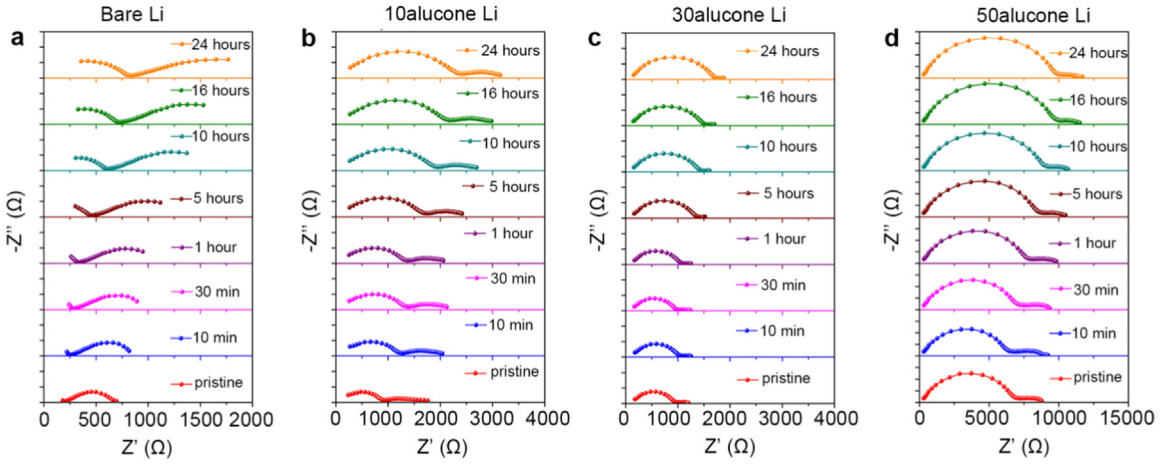

Fig. 3. Electrochemical impedance spectra of Li symmetric cells. (a) Time-dependent EIS spectra of bare Li-LSPS-Li. (b) Time-dependent EIS spectra of 10alucone Li-LSPS-Li. (c) Time-dependent EIS spectra of 30alucone Li-LSPS-Li. (d) Time-dependent EIS spectra of 50alucone Li-LSPS-Li.

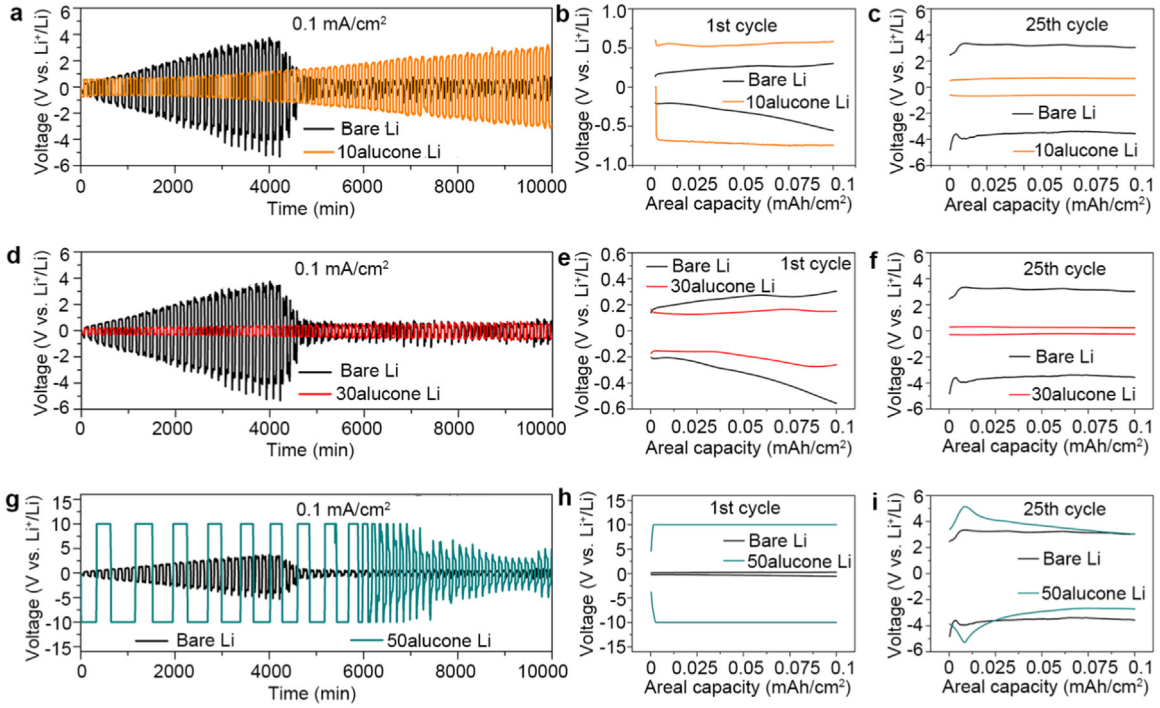

Fig. 4. Comparison of Li^+ platting/stripping behavior of Li symmetric cells at a current density of 0.1 mA cm^{-2} with an areal capacity of 0.1 mAh cm^{-2}. (a) 10 cycles alucone (10alucone Li) versus bare Li. (b, c) Voltage profiles of the 10alucone Li and the bare Li foil in the 1st cycle and the 25th cycle, respectively. (d) 30 cycles alucone (30alucone Li) versus bare Li. (e, f) Voltage profiles of the 30alucone Li and the bare Li foil in the 1st cycles and the 25th cycle, respectively. (g) 50 cycles alucone (50alucone Li) versus the bare Li. (h, i) Voltage profiles of the 50alucone Li and the bare Li foil in the 1st cycle and the 25th cycle, respectively.

stripping almost keeps less than 0.5 V within 10,000 min (Fig. 4d), strongly indicating the stable electrochemical process at the anode interface between Li metal and LSPS. Again no short circuit appears. These results are nicely consistent with EIS results above-mentioned. Compared the Li^+ platting/stripping plateau at the first cycle and 25th cycle, it also can be clearly seen that the over-potential is much lower than the that of the control sample, as shown in Fig. 4e and f. To gain insight into the chemical valent evolution of Sn in LSPS, X-ray photoelectron spectroscopy (XPS) was conducted after 25 cycles. As displayed in Fig. S6, the Sn 3d spectra exhibited spin-orbit doublet peaks at 486.76 eV ($Sn^{4+}3d_{5/2}$) and 495.22 eV (Sn^{4+} $3d_{3/2}$). [33] Without any coating, the main peaks shift to low binding energy, indicating that Sn^{4+} was reduced to Sn^{2+}. [33] With 30alucone coating, the main peaks of Sn 3d stay at the same energy position as those of pristine LSPS. The XPS results strongly suggest that MLD coating can effectively overcome the interfacial reactions between LSPS and Li metal.

When the MLD coating cycles increase to 50 cycles, there is a large over-potential at the very beginning, as present in Fig. 4g, indicating that 50alucone thin film is too thick for Li^+ hopping during the initial platting and stripping process (Fig. 4h). Interestingly, the over-potential is decreased after 10 cycles and reach the same level at the 25 cycles(Fig. 3(i)), which means the alucone layer could be lithiated, serving as artificial SEI. In addition, the alucone thin film is electronically insulative, thus the interfacial reactions between Li and LSPS can be totally suppressed as long as the thickness is optimized.

To demonstrate the necessity to build an inorganic-organic hybrid coating, purely inorganic Al_2O_3 with different thickness was also deposited by ALD on Li metal surface with TMA and water as a comparison. EIS spectra of the symmetric cells were recorded as a function of time (Fig. S7). The interface between LSPS and Li metal with 10 or 25

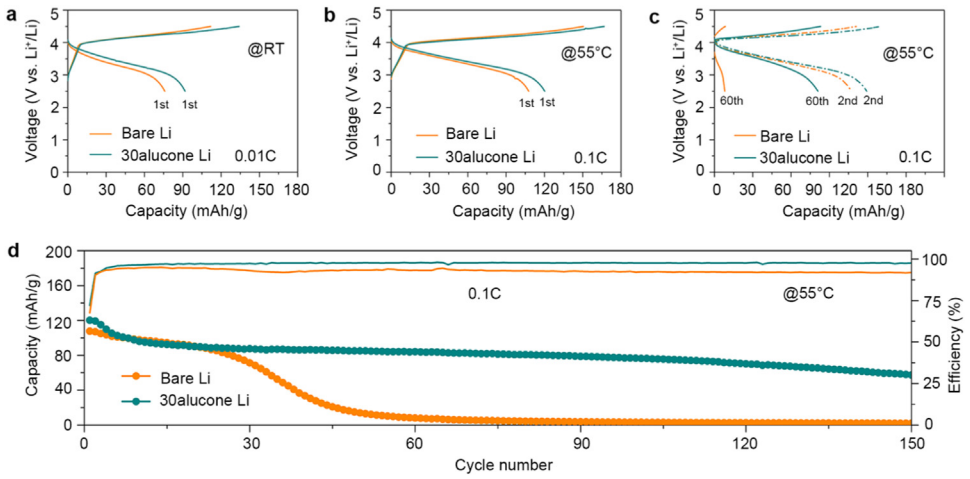

Fig. 5. Electrochemical performance of all-solid-state lithium metal batteries. (a) Initial charge-discharge curves of $LiCoO_2$-based ASSLMBs at 0.01 C at room temperature. (b) Initial charge-discharge curves of $LiCoO_2$-based ASSLMBs at 0.1 C at 55 °C. (c) Charge-discharge curves of $LiCoO_2$-based ASSLMBs at the 2nd and 60th cycles. (d) Cycle performance of $LiCoO_2$-based ASSLMBs at 55 °C.

cycles Al_2O_3 is a mixed ion-electron conductor interphase, while the interface is an ion-conducting interphase in the case of 50 and 200 cycles Al_2O_3. The results confirm that the thickness of the coating layer also plays an important role in forming different categories of the interface layer.

Furthermore, Li symmetrical cells with Al_2O_3-coated Li were also charged and discharged at a constant current density of 0.1 mA cm^{-2} (Fig. S8). The over-potential of Li^+ platting/stripping still keeps increasing over time, indicating the interfacial reactions between Li and LSPS were not well inhibited. The underlying reason is believed to be that Li-ion conductive $LiAlO_x$ thin film, which is resulted from the lithiation of Al_2O_3, [34,35] possesses a very high elastic modulus. Therefore, the $LiAlO_x$ thin film cannot accommodate the large stress/strain caused by Li^+ platting/stripping. Comparatively, organic-inorganic hybrid coating layer deposited by MLD (alucone) is much more effective than organic coating layer (Al_2O_3) deposited by ALD in terms of the suppression of lithium dendrites and interfacial reactions.

Coupled with the $LiCoO_2$ cathode, ASSLMBs were fabricated with the bare Li metal anode and 30alucone Li metal anode, respectively. First, ASSLMBs were cycled at room temperature with a current density of 0.01 C (1 C = 140 mA/g). It is clearly shown that ASSLIBs with 30alucone Li shows smaller polarization and higher initial efficiency (98%) compared to those with bare Li metal (92%) (Fig. 5a). This coincides with the EIS and Li symmetric cell results discussed above. Moreover, to increase the current density, ASSLMBs were further tested at 55 °C at 0.1 C. ASSLMBs with 30alucone Li show a specific capacity of 120 mAh/g, which is higher than that of ASSLMBs with bare Li (107 mAh/g) (Fig. 5b). After 60 cycles, ASSLMBs with bare Li metal show almost no capacity and surprisingly large polarization(Fig. 5c), which is believed to be caused by the large interfacial resistance at the anode interface. As a sharp comparison, ASSLMBs with 30 alucone Li shows smaller polarization at the 60th cycle and can be stably cycled over 150 cycles. The capacity still remains at 60 mAh/g after 150 cycles (Fig. 5d). Obviously, the improved cycle performance is resulted from the improved anode interface by MLD coating. Interestingly, the low initial efficiency jumped to 98% after several cycles, which means that a part of Li consumed to lithiate the alucone thin film during the initial charge process, forming an artificial SEI.

4. Conclusions

Li metal is regarded as the ultimate choice of ASSLMBs because of the high capacity and lowest electrochemical potential of Li metal, which enable the solid-state lithium batteries with high energy density. However, the interfacial instability of LSPS and Li metal imposes a big barrier for its application in ASSLMBs. In this work, we use MLD to develop an inorganic-organic interlayer (alucone) at the interface between Li and LSPS. With the help of the alucone coating layer, the interfacial reactions between Li metal and LSPS are greatly suppressed. In addition, lithium dendrite formation is also inhibited. By XPS analysis, the reduction of Sn^{4+} in LSPS was restrained with the MLD coating layer. Compared with bare Li, $LiCoO_2$-based ASSLMBs with 30aluocne Li exhibit smaller polarization, higher Coulombic efficiency, higher capacity, and longer cycle life. This demonstration clearly suggests that Li metal with MLD coating can be successfully applied to ASSLMBs without compromising the output voltage and energy density of ASSLMBs.

Acknowledgments

This work was supported by Natural Sciences and Engineering Research Council of Canada (NSERC), Canada Research Chair Program (CRC), China Automotive Battery Research Institute, Canada Foundation for Innovation (CFI), the Canada Light Source at University of Saskatchewan (CLS) and University of Western Ontario.

Author contribution

C. W., Y. Z., and Q. S. conceived the idea and designed the experiments. X. S. directed the project. R. L help with purchasing chemicals and characterizations. Y. L., J. L., X. L., and X. L help in data analysis. C. W. wrote the manuscript. All authors discussed the results and commented the manuscript.

Declaration of Interests

The authors declare no competing interests.

Appendix A. Supplementary material

Supplementary data associated with this article can be found in the online version at doi:10.1016/j.nanoen.2018.08.030.

References

[1] S. Xin, Y. You, S. Wang, H.-C. Gao, Y.-X. Yin, Y.-G. Guo, ACS Energy Lett. 2 (2017) 1385–1394.
[2] C. Sun, J. Liu, Y. Gong, D.P. Wilkinson, J. Zhang, Nano Energy 33 (2017) 363–386.
[3] X. Yu, A. Manthiram, Acc. Chem. Res. 50 (2017) (2653-2600).
[4] A. Manthiram, X. Yu, S. Wang, Nat. Rev. Mater. 2 (2017) 16103.
[5] Y. Kato, S. Hori, T. Saito, K. Suzuki, M. Hirayama, A. Mitsui, M. Yonemura, H. Iba, R. Kanno, Nat. Energy 1 (2016) 16030.
[6] K. Xu, Chem. Rev. 104 (2004) 4303–4418.
[7] D. Lin, Y. Liu, Y. Cui, Nat. Nano 12 (2017) 194–206.
[8] N.-W. Li, Y.-X. Yin, C.-P. Yang, Y.-G. Guo, Adv. Mater. 28 (2016) 1853–1858.
[9] N. Ohta, K. Takada, L. Zhang, R. Ma, M. Osada, T. Sasaki, Adv. Mater. 18 (2006)

2226–2229.
[10] T. Kobayashi, A. Yamada, R. Kanno, Electrochim. Acta 53 (2008) 5045–5050.
[11] X. Yao, N. Huang, F. Han, Q. Zhang, H. Wan, J.P. Mwizerwa, C. Wang, X. Xu, Adv. Energy Mater. 7 (2017) 1602923.
[12] Z. Zhang, Y. Zhao, S. Chen, D. Xie, X. Yao, P. Cui, X. Xu, J. Mater. Chem. A 5 (2017) 16984.
[13] W. Luo, Y. Gong, Y. Zhu, Y. Li, Y. Yao, Y. Zhang, K. Fu, G. Pastel, C.-F. Lin, Y. Mo, E.D. Wachsman, L. Hu, Adv. Mater. 29 (2017) 1606042.
[14] K. Fu, Y. Gong, B. Liu, Y. Zhu, S. Xu, Y. Yao, W. Luo, C. Wang, S.D. Lacey, J. Dai, Y. Chen, Y. Mo, E. Wachsman, L. Hu, Sci. Adv. 3 (2017) e1601659.
[15] A.C. Kozen, C.-F. Lin, A.J. Pearse, M.A. Schroeder, X. Han, L. Hu, S.-B. Lee, G.W. Rubloff, M. Noked, ACS Nano 9 (2015) 5884–5892.
[16] Z. Zhang, S. Chen, J. Yang, J. Wang, L. Yao, X. Yao, P. Cui, X. Xu, ACS Appl. Mater. Interfaces 10 (2017) 2556–2565.
[17] X. Han, Y. Gong, K. Fu, X. He, G.T. Hitz, J. Dai, A. Pearse, B. Liu, H. Wang, G. Rubloff, Y. Mo, V. Thangadurai, E.D. Wachsman, L. Hu, Nat. Mater. 16 (2017) 572–579.
[18] Y. Zhu, X. He, Y. Mo, Adv. Sci. 4 (2017) 1600517.
[19] X. Li, A. Lushington, Q. Sun, W. Xiao, J. Liu, B. Wang, Y. Ye, K. Nie, Y. Hu, Q. Xiao, R. Li, J. Guo, T.-K. Sham, X. Sun, Nano Lett. 16 (2016) 3545–3549.
[20] Y. Zhao, L.V. Goncharova, Q. Zhang, P. Kaghazchi, Q. Sun, A. Lushington, B. Wang, R. Li, X. Sun, Nano Lett. 17 (2017) 5653–5659.
[21] Z. Yang, G.L. V, S. Qian, L. Xia, L. Andrew, W. Biqiong, L. Ruying, D. Fang, C. Mei, S. Xueliang, Small Methods 0 (2018) 1700417.
[22] L. Yue, J. Ma, J. Zhang, J. Zhao, S. Dong, Z. Liu, G. Cui, L. Chen, Energy Storage Mater. 5 (2016) 139–164.
[23] X.B. Cheng, R. Zhang, C.Z. Zhao, F. Wei, J.G. Zhang, Q. Zhang, Adv. Sci. 3 (2015) 1500213.
[24] B.H. Lee, B. Yoon, V.R. Anderson, S.M. George, J. Phys. Chem. C. 116 (2012) 3250–3257.
[25] S.P. Ong, Y. Mo, W.D. Richards, L. Miara, H.S. Lee, G. Ceder, Energy Environ. Sci. 6 (2013) 148–156.
[26] P. Bron, S. Johansson, K. Zick, J. Schmedt auf der Günne, S. Dehnen, B. Roling, J. Am. Ceram. Soc. 135 (2013) 15694–15697.
[27] C. Vinado, S. Wang, Y. He, X. Xiao, Y. Li, C. Wang, J. Yang, J. Power Sources (2018), https://doi.org/10.1016/j.jpowsour.2018.1006.1038.
[28] Y. Wang, W.D. Richards, S.P. Ong, L.J. Miara, J.C. Kim, Y. Mo, G. Ceder, Nat. Mater. 14 (2015) 1026–1031.
[29] J.C. Bachman, S. Muy, A. Grimaud, H.-H. Chang, N. Pour, S.F. Lux, O. Paschos, F. Maglia, S. Lupart, P. Lamp, L. Giordano, Y. Shao-Horn, Chem. Rev. 116 (2016) 140–162.
[30] P. Bron, B. Roling, S. Dehnen, J. Power Sources 352 (2017) 127–134.
[31] J. Jamnik, J. Maier, S. Pejovnik, Electrochim. Acta 44 (1999) 4139–4145.
[32] X.-B. Cheng, R. Zhang, C.-Z. Zhao, Q. Zhang, Chem. Rev. 117 (2017) 10403–10473.
[33] Y. Sohn, J. Am. Ceram. Soc. 97 (2014) 1303–1310.
[34] S.C. Jung, H.-J. Kim, J.W. Choi, Y.-K. Han, Nano Lett. 14 (2014) 6559–6563.
[35] Y. Zhao, L.V. Goncharova, A. Lushington, Q. Sun, H. Yadegari, B. Wang, W. Xiao, R. Li, X. Sun, Adv. Mater. 29 (2017) 1606663.

Changhong Wang is currently a Ph.D. candidate in Prof. Xueliang (Andy) Sun's Group at the University of Western Ontario, Canada. He got his B.S. in applied chemistry from University of Science and Technology of Anhui in 2011 and obtained his M.S. degree in materials engineering from University of Science and Technology of China in 2014. After graduation, he also served as a research assistant in Singapore University of Technology and Design from 2014 to 2016. Currently, his research interests include solid-state sulfide electrolytes, all-solid-state LIBs and Li-S batteries, and memristors.

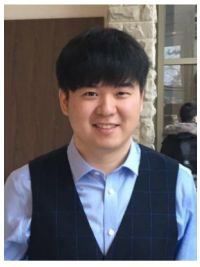

Yang Zhao is currently a Ph.D. candidate in Prof. Xueliang (Andy) Sun's Group at the University of Western Ontario, Canada. He received his B.S. degree and M.S. degree in Chemical Engineering and Technology from Northwestern Polytechnical University (Xi'an, China) in 2011 and 2014, respectively. His current research interests focus on atomic/molecular layer deposition in the application of lithium/sodium ion batteries and all solid state batteries.

Dr. Qian Sun is a postdoctoral associate in Prof. Xueliang (Andy) Sun's Group at the University of Western Ontario (Western Univerisity), Canada. He received his B.S. degree in Chemistry in 2006, M.S. degree in Physical Chemistry in 2009, and Ph.D. degree in Applied Chemistry in 2013 under the supervision of Prof. Dr. Zheng-Wen Fu on the study of Li-/Na-ion batteries and Na-air batteries, all at Fudan University, China. He joined Prof. Sun's group in 2013 and his current research interests focus on Na-air, Na-ion, and room temperature Na-S batteries as well as solid-state Li/Na batteries.

Dr. Xia Li is a postdoctoral fellow in Prof. Xueliang (Andy) Sun's Nanomaterials and Energy Group. She received her Ph.D. degree at the University of Western Ontario, Canada. Her current research interests focus on the development of advanced nanomaterials for lithium-sulfur batteries, sulfide-based solid-state electrolytes.

Dr. Yulong Liu is currently a postdoctoral fellow in Prof. Xueliang (Andy) Sun' Nanomaterials and Energy Group at the University of Western Ontario, Canada. He received his Bachelor degree from Central South University, China, in 2010, and Master degree in 2013. In 2017, he obtained his Ph.D. degree in Materials Science and Engineering from University of Western Ontario. His research interests include nanomaterials for lithium-ion batteries, especially LiFePO4 (in collaboration with Johnson Matthey Inc., previous Phostech), and the development of the solid state batteries.

Dr. Jianwen Liang received his Ph.D. degree in inorganic chemistry from University of Science and Technology of China in 2015. He is currently a postdoctoral fellow in Prof. Xueliang (Andy) Sun' Nanomaterials and Energy Group at the University of Western Ontario, Canada. His research interests include sulfide-based solid-state electrolyte as well as all-solid-state Li/Li-ion batteries.

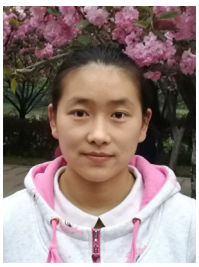

Dr. Xiaona Li is a postdoctoral associate in Prof. Xueliang (Andy) Sun's Group at the University of Western Ontario (Western Univerisity), Canada. She received her B.S. degree in Material Chemistry in 2011 from Sichuan University and Ph.D. degree in Inorganic Chemistry in 2015 under the supervision of Prof. Dr. Yitai Qian on the study of electrode materials synthesis for Li+ /Na+ batteries from University of Science and Technology of China. She joined Prof. Sun's group in 2017 and her current research interests focus on the synthesis of sulfide solid electrolytes and all-solid-state batteries.

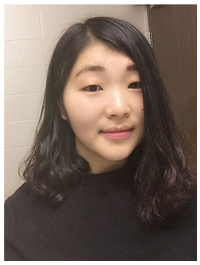

Xiaoting Lin is currently a Ph.D. candidate in Prof. Xueliang (Andy) Sun's group at the University of Western Ontario, Canada. She received her B.S. degree in Applied chemistry in 2012 from Liaocheng University and obtained her M.S. degree in Physical Chemistry in 2016 from Ningbo University. Currently, her research interests focus on the development of advanced nanomaterials for Na-O2 batteries as well as solid-state Na-O2 batteries.

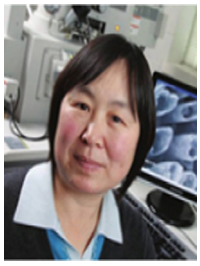

Ruying Li is a research engineer at Prof. Xueliang (Andy) Sun's Nanomaterial and Energy Group at the University of Western Ontario, Canada. She received her master in Material Chemistry under the direction of Prof. George Thompson in 1999 at University of Manchester, UK, followed by work as a research assistant under the direction of Prof. Keith Mitchell at the University of British Columbia and under the direction of Prof. Jean-Pol Dodelet at l'Institut national de la recherché Scientifique (INRS), Canada. Her current research interests are associated with synthesis and characterization of nanomaterials for electrochemical energy storage and conversion.

Keegan Adair received his B.Sc. in chemistry from the University of British Columbia in 2016. He is currently a Ph.D. candidate in Prof. Xueliang (Andy) Sun's Nanomaterials and Energy Group at the University of Western Ontario, Canada. Keegan has previously worked on battery technology at companies such as E-One Moli Energy and General Motors. His research interests include the design of nanomaterials for lithium metal batteries and nanoscale interfacial coatings for battery applications.

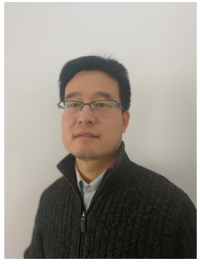

Dr. Li Zhang is currently a senior scientist of China Automotive Battery Research Institute Co., Ltd., Beijing, China. He received his Ph.D. degree in Electrochemistry from University of Science & Technology Beijing , China in 2009. He has more than 10 years of power sources experience with expertise in battery materials as well as electrode design. Currently, his research interests include solid-state electrolytes, all-solid-state Li-air, and lithium batteries.

Dr. Rong Yang received his Ph.D. degree in inorganic chemistry from Peking University in 2011. He is currently a senior engineer in China Automotive Battery Research Institute. His research interests are focused on cathode materials for lithium-ion batteries, solid-state lithium ion conductors, and solid-state lithium-ion batteries.

Dr. Shigang Lu is Vice president of China Automotive Battery Research Institute Co., Ltd. He has the responsibility for technology innovations in the area of automotive battery application. He has extensive experience in many energy research areas including fuel cells, and lithium-ion batteries. Dr. Lu received her Ph.D. degree in Chemistry from Moscow State University in 1993. He has extensive experience in novel material processing techniques for automotive battery applications. His current research interests include new energy electrochemistry, lithium-ion battery and related materials, solid-state battery and related materials.

Prof. Xueliang (Andy) Sun is a Canada Research Chair in Development of Nanomaterials for Clean Energy, Fellow of the Royal Society of Canada and Canadian Academy of Engineering and Full Professor at the University of Western Ontario, Canada. Dr. Sun received his Ph.D. in materials chemistry in 1999 from the University of Manchester, UK, which he followed up by working as a postdoctoral fellow at the University of British Columbia, Canada and as a Research Associate at L'Institut National de la Recherche Scientifique (INRS), Canada. His current research interests are focused on advanced materials for electrochemical energy storage and conversion, including electrocatalysis in fuel cells and electrodes in lithium-ion batteries and metal-air batteries.